Inorganic Chemistry

Article

pubs.acs.org/IC

The Syntheses and Electrochemical Studies of a Ferrocene Substituted Diiminopyridine Ligand and Its P, S, Se, and Te Complexes

Eleanor Magdzinski, Pierangelo Gobbo, Caleb D. Martin, Mark S. Workentin, and Paul J. Ragogna*

Department of Chemistry and The Centre for Advanced Materials and Biomaterials Research (CAMBR), Western University, 1151 Richmond St., London ON, N6A 5B7, Canada

Supporting Information

ABSTRACT: A new reversible, redox active diiminopyridine ligand (**1Fc**) containing pendant ferrocene functionalities was isolated and fully characterized. The reaction of **1Fc** with chalcogen pseudohalides of sulfur, selenium, and tellurium yielded the respective *N*,*N*′,*N*″-chelated chalcogen dications. Phosphorus chemistry proceeded in a related manner but, in this case, by the direct addition of **1Fc** with PI_3 to yield the *N*,*N*′,*N*″-chelated P(I) cation. These species represent the first synthesized main group complexes involving a redox active diiminopyridine ligand containing pendant ferrocenes. Electrochemical studies of the free ligand shows a reversible two-electron process. The chelated phosphorus cation, however, displayed three events, the first being a quasi-reversible two-electron process, involving the oxidation at the P(I) center, resulting in a P(III) cation. The subsequent reversible one- and two-electron processes arise from the ligand framework and pendant ferrocenes, respectively.

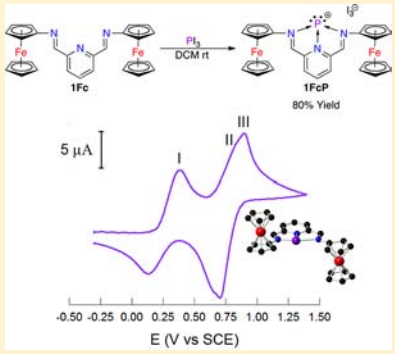

INTRODUCTION

In the past decade, there has been an interest in synthesizing monocationic and polycationic main group centered molecules to study the nature of their structure, bonding, and reactivity. Although there are a variety of synthetic methods used to produce these species, nitrogen-based ligands have been the dominant support for the cations.[1,2] Many of the reports have focused on producing novel complexes using ligands where the substituents (alkyl or aryl) can be varied within the ligand framework; however, examples of these common supports that feature pendant redox active (i.e., ferrocene) fragments are relatively rare (Figure 1). It is known that transition metal based complexes containing redox active ligands or ligands substituted with redox active components have been used in a diverse array of applications including catalysis, optical materials, or in the manufacture of biological sensors.[3−5] The appeal of ligands with redox active functional groups stems from their ability to change the electronic properties of the central metal without the need for further synthetic modifications. This occurs by either varying an applied potential or introducing a chemical redox agent into a reaction, whereby an oxidation or reduction at ferrocene has the ability to "turn on" or "turn off" a particular molecule. Imparting redox active species onto a ligand offers exciting opportunities within homogeneous transition metal catalysts, as the oxidation of the redox active substituent induces a higher electrophilicty and, therefore, a change in reactivity of a catalytically active transition metal center.[6] In many cases, these ligands exhibit reversible redox processes and therefore enable "switchable" control of the electronic properties of a central metal.

The synthesis and reactivity of nitrogen-based ligands containing ferrocene pendant to the ligand framework have appeared in the literature, but their chemistry largely remains unexplored. Of the few examples reported, studies have been limited to metals of the d block. Stephan et al. synthesized ferrocenyl amidinates of Ti or Zr in order to study these ligands as possible redox tunable olefin polymerization catalysts (Figure 1, **I** and **II**).[7] In another report, a bis-ferrocenyl-β-diketiminate was synthesized and used to prepare Zn complexes that revealed unusual "non-innocent" reactivity at the β-diketiminate ligand as opposed to the transition metal center (Figure 1, **III** and **IV**).[8] Bildstein et al. has focused their efforts in synthesizing a ferrocene containing 1,4-diaza-1,3-butadiene ligand for the preparation of Cr, Mo, and W complexes, with the intention of producing redox tunable olefin polymerization catalysts (Figure 1, **V**).[9] Gibson et al. has synthesized a diiminopyridine (DIMPY) ligand to complex Fe and Co centers, again with an eye toward effective switchable catalysts for olefin polymerization (Figure 1, **VI**).[10] Another example by this group utilizes the bis(iminophenoxide) ligand framework and modifies it in such a way as to contain ferrocene moieties. The resulting Ti complex (Figure 1, **VII**) was used to show that activity can indeed be varied by redox switching of the ferrocenyl unit contained within the ligand backbone of a lactide polymerization catalyst by introduction of a chemical redox agent.[11]

Recently, the nitrogen-based ligand set, diiminopyridine (Figure 1, R-DIMPY), has been featured prominently in the

Received: May 10, 2012
Published: July 9, 2012

dx.doi.org/10.1021/ic300974u | *Inorg. Chem.* 2012, 51, 8425−8432

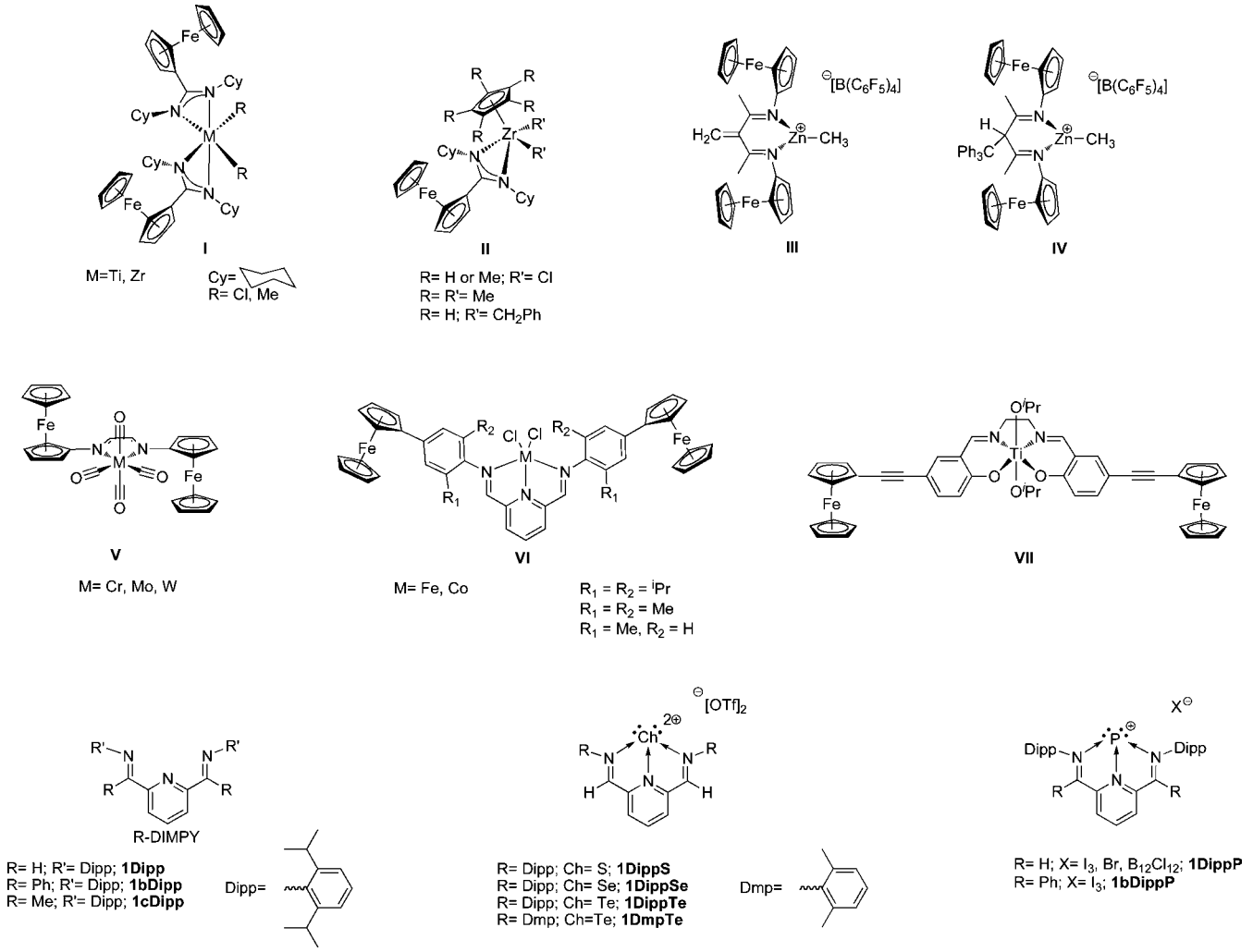

Figure 1. A few known nitrogen-based ligand complexes with ferrocenyl and nonferrocenyl substituents.

isolation of cationic main group species.[12−21] Our group has utilized the *N,N'*-aryl substituted versions to stabilize low valent dicationic chalcogen (Figure 1, **1DippS**, **1DippSe**, **1DippTe**, and **1DmpTe**)[22] or monocationic phosphorus (Figure 1, **1DippP** and **1bDippP**)[23] centers; however, there are no reports of utilizing nitrogen-based ligands that feature redox active substituents in the stabilization of highly novel main group cations.

In this context, we report the synthesis, characterization, and electrochemical behavior of a new DIMPY ligand (**1Fc**), containing pendant ferrocenyl fragments on the imine nitrogens (Scheme 1, **A**). We have explored its reactivity with main group metals from groups 15 (P) and 16 (S, Se, Te), and furthermore, the electrochemistries of these compounds have been investigated. The electrochemical studies reveal the possibility of generating the putative tricationic phosphorus centered species, and under the conditions employed this indicates that the polycation may be isolable. These results represent the first inroads into such redox active main group compounds.

RESULTS AND DISCUSSION

Synthesis. *N,N'*-Diferrocenyl diiminopyridine (FcDIMPY; **1Fc**) was prepared by the condensation reaction between 1-aminoferrocene and 2,6-pyridinedialdehyde[30] in a 2:1 stoichiometry under an ethanol reflux (Scheme 1, **A**). A dark red-purple powder precipitated and was isolated using vacuum filtration. The solids were washed with cold ethanol and dried, and a sample of the bulk powder was redissolved in $CDCl_3$. The ^1H NMR spectrum indicated the presence of six distinct signals: three in the aromatic region, consistent with protons on the DIMPY framework, and three for the monosubstituted ferrocene species that appeared to shift downfield relative to the aminoferrocene starting material (Table 1).

A solution of **1Fc** in DCM was stirred with one stoichiometric equivalent of the appropriate chalcogen pseudohalide starting material (**S**$(OTf)_2$, CyDAB**Se**OTf_2, and $Dipp_2$BIAN**Te**OTf_2) in the same solvent at room temperature (Scheme 1, **B**). In all cases, color changes from orange-red to a dark blue-green were immediately observed. Normal pentane and Et_2O were used to precipitate out the dark blue-green solids, which were then dried *in vacuo*. Proton NMR spectra of the redissolved solids in CD_3CN revealed downfield shifts (Table 1) for all resonances relative to the free ligand, indicative of coordination of the ligand to an electron deficient chalcogen center. These compounds were tentatively assigned as the salts **1FcS**, **1FcSe**, and **1FcTe**. X-ray quality crystals of all compounds were grown, and subsequent X-ray diffraction experiments confirmed the identity of the solids, which were isolated in 65−80% yields.

dx.doi.org/10.1021/ic300974u | *Inorg. Chem.* 2012, 51, 8425−8432

Scheme 1. Synthetic Routes to 1Fc, 1FcS, 1FcSe, 1FcTe, and 1FcP

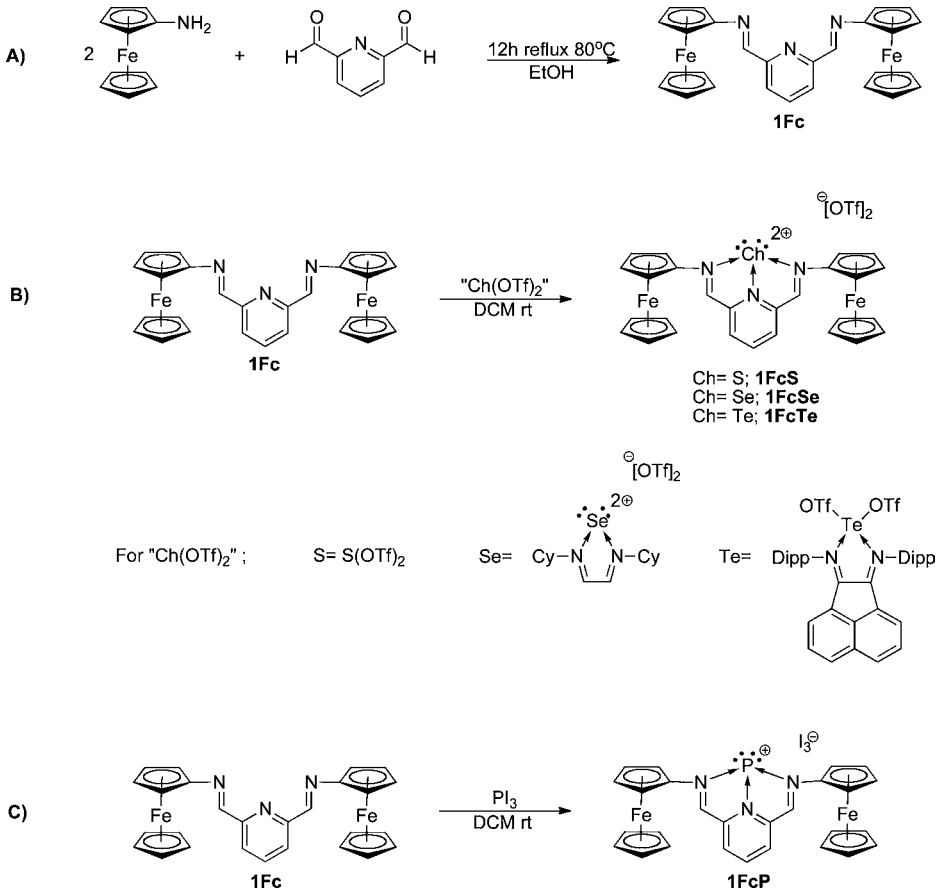

Table 1. ^{1}H NMR Chemical Shifts (ppm) for 1Fc, 1FcS, 1FcSe, 1FcTe, and 1FcP

compound	1Fc	1FcS	1FcSe	1FcTe	1FcP
δ_H imine, 2H	8.81	10.07	10.14	10.32	9.52
δ_H py-*d*, 2H	8.21	9.02	8.94	8.84	8.63
δ_H py-*t*, 1H	7.84	8.84	8.85	8.73	7.12
δ_H H_a-*pt*, 2H	4.71	5.52	5.55	5.55	5.52
δ_H H_b-*pt*, 2H	4.35	5.18	5.15	5.07	4.86
δ_H H_c-*s*, 10H	4.21	4.53	4.52	4.48	4.57

The 1:1 stoichiometric addition of **1Fc** with PI_3 underwent a similar color transformation as was observed in the formation of the chalcogen salts (Scheme 1, **C**). Approximately 10 min after the addition of **1Fc** to PI_3, the reaction mixture was sampled and analyzed by $^{31}P\{^1H\}$ NMR spectroscopy, which showed the disappearance of the signal for free PI_3 (δ_P = 178) and formation of a single phosphorus peak at δ_P = 123.99. This shift corresponds with other reported P(I) DIMPY complexes previously.[23] A solid green-black product was precipitated by the addition of a combination of *n*-pentane and Et_2O. The corresponding ^{1}H NMR spectrum of the redissolved solids in CD_2Cl_2 showed a diagnostic doublet for the imine protons (δ_H = 9.52; $^3J_{PH}$ = 2.8 Hz), indicative of the successful incorporation of phosphorus into the ligand framework.

On the basis of these multinuclear NMR spectroscopic data, the compound was tentatively assigned as being the DIMPY complex of the phosphorus salt **1FcP**. For further verification, suitable crystals for X-ray diffraction were grown, and subsequent diffraction experiments confirmed the identity of the compound as **1FcP**.

X-Ray Crystallography. The solid-state structure obtained from X-ray diffraction studies on single crystals of **1Fc**

Table 2. Selected Bond Lengths (Å) and Bond Angles (deg) for 1FcS, 1FcSe, 1FcTe, and 1FcP and their analogues 1DippS, 1DippSe, 1DippTe, and 1DippP

	1FcS	1DippS[22]	1FcSe	1DippSe[22]	1FcTe	1DippTe[22]	1FcP	1DippP[23]
E(1)–N(1)	1.922(5)	1.9068(17)	2.068(2)	2.025(9)	2.230(3)	2.243(4)	2.275(4)	1.877(7)
E(1)–N(2)	1.709(7)	1.719(3)	1.872(2)	1.872(3)	2.068(3)	2.098(3)	1.725(5)	1.722(6)
E(1)–N(3)	1.922(5)[a]	1.9068(17)[a]	2.086(9)	2.025(9)[a]	2.208(3)	2.241(4)	1.777(4)[a]	1.975(8)
C(1)–N(1)	1.287(8)	1.280(3)	1.291(3)	1.275(3)	1.286(5)	1.284(6)	1.314(5)	1.303(11)
C(7)–N(3)	1.287(8)[a]	1.280(3)[a]	1.284(3)	1.275(3)[a]	1.308(5)	1.284(7)	1.314(5)[a]	1.316(11)
N(1)–E(1)–N(2)	82.60(17)	82.39(6)	79.22(9)	78.79(6)	73.81(12)	72.77(15)	73.90(11)	81.6(3)
N(2)–E(1)–N(3)	82.60(17)[a]	82.39(6)[a]	78.43(9)	78.79(6)[a]	74.42(12)	73.35(16)	88.52(14)	81.1(3)

[a]Symmetry arising from the centrosymetric nature of those marked compounds.

dx.doi.org/10.1021/ic300974u | Inorg. Chem. 2012, 51, 8425–8432

Table 3. X-Ray Details for 1Fe, 1FcS, 1FcSe, 1FcTe, and 1FcP

compound	1Fc	1FcS	1FcSe	1FcTe	1FcP
empirical formula	$C_{31}H_{31}Fe_2N_3O_1$	$C_{29}H_{23}F_6Fe_2N_3O_6S_3$	$C_{29}H_{23}F_6Fe_2N_3O_6S_2Se_1$	$C_{29}H_{23}F_6Fe_2N_3O_6S_2Te_1$	$C_{27}H_{23}Fe_2I_3N_3P_1$
FW (g/mol)	573.29	831.38	878.28	926.92	912.85
cryst syst	triclinic	monoclinic	triclinic	triclinic	monoclinic
space group	$P\bar{1}$	$C2/c$	$P\bar{1}$	$P\bar{1}$	$C2/c$
a (Å)	11.2926(16)	12.970(2)	10.7138(9)	10.732(3)	12.0077(10)
b (Å)	11.6402(17)	18.528(3)	11.5291(9)	11.537(3)	17.2096(14)
c (Å)	12.1762(17)	13.477(2)	13.6160(11)	13.662(4)	13.8818(11)
α (deg)	68.139(3)	90.000	104.007(2)	103.487(6)	90.000
β (deg)	72.717(3)	109.608(4)	94.864(3)	94.198(7)	99.153(2)
γ (deg)	61.101(3)	90.000	107.862(2)	106.741(6)	90.000
V (Å^3)	1286.9(3)	3050.8(8)	1530.0(2)	1557.2(7)	2832.1(4)
Z	2	4	2	2	4
D_c (mg m^{-3})	1.479	1.810	1.906	1.977	2.141
radiation, λ (Å)	0.71073	0.71073	0.71073	0.71073	0.71073
temp (K)	150(2)	150(2)	150(2)	150(2)	150(2)
$R1[I > 2\sigma I]^a$	0.0604	0.0706	0.0325	0.0407	0.0343
$wR2(F^2)^a$	0.1695	0.1586	0.0792	0.0882	0.0740
GOF(S)^a	1.022	1.102	1.029	1.054	1.085

$^a R1(F[I > 2(I)]) = \sum||F_o| - |F_c||/\sum|F_o|$; $wR2(F^2\ [\text{all data}]) = [w(F_o^2 - F_c^2)^2]^{1/2}$; $S(\text{all data}) = [w(F_o^2 - F_c^2)^2/(n-p)]^{1/2}$ (n = no. of data; p = no. of parameters varied; $w = 1/[^2(F_o^2) + (aP)^2 + bP]$, where $P = (F_o^2 + 2F_c^2)/3$ and a and b are constants suggested by the refinement program.

Table 4. Solid-State Structures of 1Fc, 1FcS, 1FcSe, 1FcTe, and 1FcP (Thermal Ellipsoids Drawn to the 50% Probability Level; Solvates and Hydrogen Atoms Removed for Clarity)

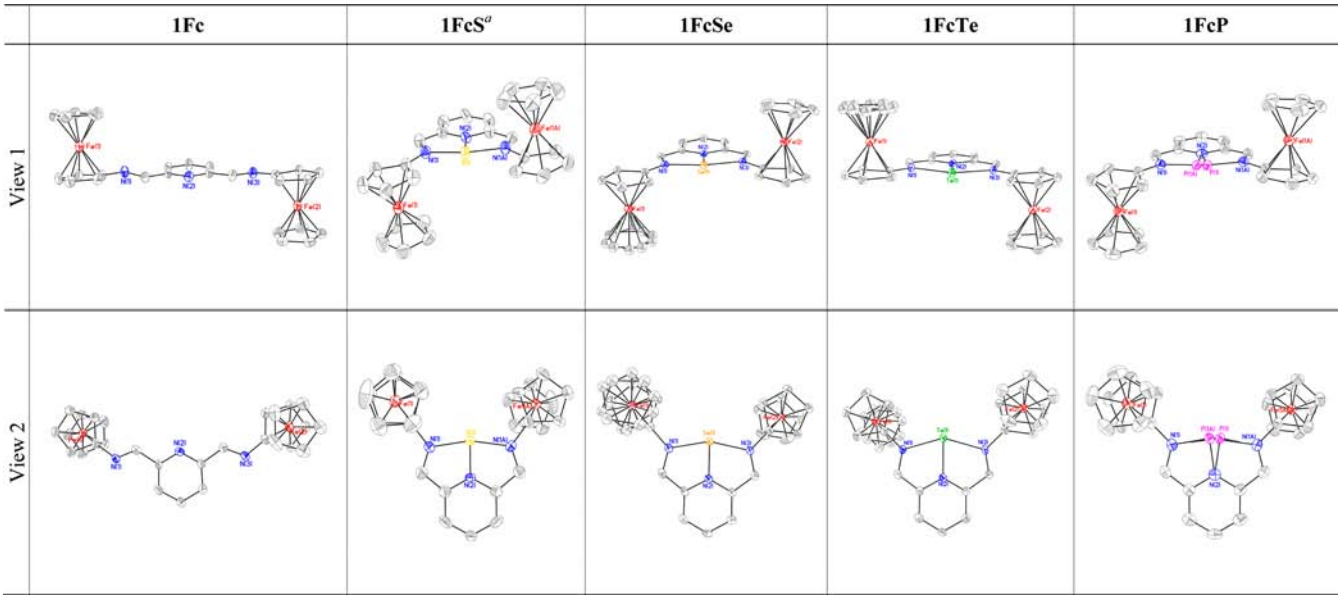

[a]Disorder removed for clarity.

confirmed the identity of a diiminopyridine ligand bearing ferrocene groups on the two nitrogen atoms (Table 4). The carbon−nitrogen double bonds are indicative of a diimine (C=N; 1.266(6) and 1.267(6)), and the remaining metrical parameters are consistent with the well-documented diiminopyridine framework.

The solid-state structures of the corresponding main group complexes of **1Fc** indicate the presence of the cationic phosphorus (**1FcP**) or dicationic chalcogen centers (**1FcS**, **1FcSe**, and **1FcTe**) within the *N*,*N*′,*N*″-DIMPY chelate (see Table 2 for salient bond lengths and angles, Table 3 for X-ray data, and Table 4 for structures). For all species, the bonding within the diiminopyridine framework has little deviation from the previously reported *N*,*N*′-diisopropylphenyl (Dipp) derivatives (Figure 1, **1DippS**, **1DippSe**, **1DippTe**, and **1DippP**),[22,23] demonstrating that the ferrocene groups do not alter the interaction between the ligand to the main group center. In contrast to the Dipp derivatives that have bulky aryl groups oriented perpendicular to the diiminopyridine plane, the ferrocene substituents in all species are coplanar with respect to the cyclopentadiene ring bound at the nitrogen and the diiminopyridine contiguous rings.

In all of the structures, the ferrocene groups are oriented *anti* to one another to minimize steric interactions, and as a result, all of the species have *pseudo*-C_2 symmetry through the E(1)−N(2)−C(4) axis (**1FcS** and **1FcP** are perfectly C_2 symmetric). Compound **1FcP** is disordered at the phosphorus center, modeled with a 50% occupancy at both sites. In the case of

dx.doi.org/10.1021/ic300974u | Inorg. Chem. 2012, 51, 8425−8432

1FcS, disorder arises from the presence of the other *anti* configuration of the complex. Compounds **1FcS** and **1FcP** lack sulfur−oxygen and phosphorus−iodine contacts within the sum of the van der Waals radii to either the triflate ($\sum_{v.d.W.}$ S−O = 3.25 Å) or the triiodide counterion ($\sum_{v.d.W.}$ P(1)−I = 5.33 Å, $\sum_{v.d.W.}$ P(1)A−I = 5.49 Å). The closest contacts in **1FcSe** and **1FcTe** between the cation and anions lie on the edge of the sum of the van der Waals radii (**1FcSe** Se···O = 3.367 Å cf. $\sum_{v.d.W.}$ Se−O = 3.42 Å; **1FcTe** Te···O = 3.068 Å cf. $\sum_{v.d.W.}$ Te−O = 3.58 Å).[24] Despite these distant contacts, all species are viewed as distinct cation−anion pairs, as there is no elongation of the related sulfur−oxygen bond in the triflate anion, indicative of ionic formulations.

Electrochemistry. Compounds **1Fc**, **1FcP**, **1DippP** (with I_3^- anion), and its free Dipp ligand (Figure 1, **1Dipp**) were characterized by cyclic voltammetry (CV) using 2 mM solutions in 5 mL of a DCM/0.1 M $TBAPF_6$ electrolyte solution. The working electrode was a 1 mm platinum disk electrode. The counter electrode was a platinum wire, and the reference electrode was a Ag/AgCl electrode. However, the voltammetric curves were all calibrated to the standard calomel electrode (SCE) using nitrobenzene as the internal standard.

Compound **1Fc** (Figure 2, A) shows a reversible peak with E° at 0.73 V related to the two ferrocene moieties. The peak

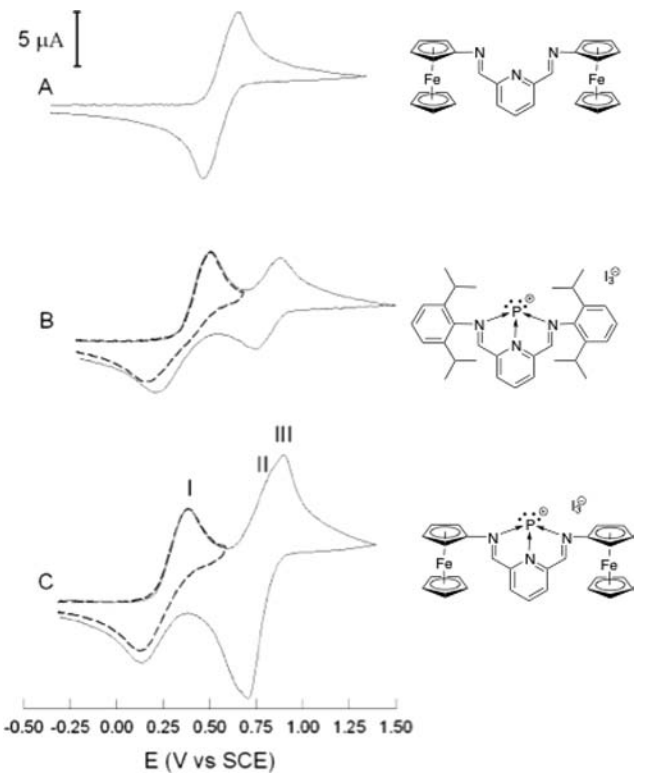

Figure 2. From top to bottom, CV of **1Fc** (A), **1DippP** (B), and **1FcP** (C) recorded at a Pt electrode in DCM/0.1 M $TBAPF_6$ with an analyte concentration of 2 mM and at 0.5 V s^{-1}. Experiment carried out inside of a glovebox at room temperature.

current is indicative of a two electron process, showing that the two ferrocenes are being oxidized at the same or similar potential, suggesting little or no electronic interaction between them, as expected due to poor conjugation within the molecule. Similar redox behavior has been observed for other *N,N′*-diferrocenyl diazabutadiene type ligands.[9] In the same potential window, compound **1FcP** shows three oxidation peaks (Figure 2, C): Peak I with $Ep_{1/2}$ at 0.36 V is quasi-reversible and is a two electron process. Peak II appearing as a shoulder overlapping with peak III is a reversible one electron process. Peak III with E° at 0.94 V is a reversible two electron process. To better understand the electrochemistry of **1FcP**, an analogous phosphorus complex **1DippP**, containing two Dipp substituents and a triiodide anion, was analyzed under identical experimental conditions. This complex (Figure 2, B) shows two distinct electrochemical processes. The first is a quasi-reversible oxidation with $Ep_{1/2}$ at 0.36 V and involves two electrons, and the second is a reversible one electron peak with E° at 0.81 V. These two signals appear when nitrogen atoms of the ligand coordinate the phosphorus and are likely related to the loss of two electrons on the P(I) forming a P(III) center during the first quasi-reversible process and the subsequent reversible oxidation of the ligand induced by complexation to P in the second one electron reversible process, as these processes are not observed in the free ligand. The complete CV of this compound (figure available in Supporting Information) shows two other irreversible peaks at 2.00 V and 2.54 V due to the oxidation of the two Dipp groups, consistent with the observed electrochemistry for the free ligand (figure available in the Supporting Information) where no other redox behavior is observed in the −0.5 to 2.0 V range.

The assignment of the voltammetric peaks I and II (Figure 2, C) obtained for the complex **1FcP** is supported by comparison with the electrochemical data obtained for the aforementioned **1DippP** derivative (Figure 2, B) where the first two oxidations are related to the coordination of the three nitrogens of the ligand to phosphorus. Peak III, the two electron reversible peak, is absent from the CV of **1DippP** and results from the oxidation of the two ferrocene groups present in **1FcP**. Relative to the free ligand (**1Fc**), this signal is shifted slightly toward more positive potentials due to a loss in electron density from the ligand framework as a result of coordinating to the electron deficient phosphorus center.

The electrochemistry of complexes **1FcS**, **1FcSe**, and **1FcTe** were also investigated by CV. However, the poor solubility of these complexes and the reactivity of these chalcogen complexes with the electrochemistry solvents and electrode materials made analysis more difficult. These compounds were found to be slightly soluble in CH_3CN/0.05 M $TBABF_4$ as an electrolyte solution. Their CVs were recorded saturating the electrolyte solution with analyte. In these cases, the working electrode was a glassy carbon (GC) disk electrode. These CVs, available in the Supporting Information, show the same general features, although broadened and less resolved as the voltammetric curve obtained for the complex **1FcP**, namely the quasi-reversible oxidation of the chalcogen-ligand followed by a two electron oxidation of the ferrocene moieties.

■ CONCLUSIONS

Compounds **1FcS**, **1FcSe**, **1FcTe**, and **1FcP** represent the first examples of group 15 and 16 salts utilizing a redox active DIMPY ligand (**1Fc**) containing pendant ferrocene functionalities. Cyclic voltammetric studies of the free ligand display a reversible two electron process with E° at 0.73 V. A full data collection for the *N,N′,N″*-chelated chalcogen complexes remains somewhat inconclusive, due to the insolubility of these complexes. An electrochemical investigation of **1FcP** was performed, showing three events: a quasi-reversible two electron process for the production of a P(III) centered cation

dx.doi.org/10.1021/ic300974u | *Inorg. Chem.* 2012, 51, 8425−8432

with $Ep_{1/2}$ at 0.36 V, a second reversible one electron process from the ligand framework which overlaps with a third two electron process from the non-communicating ferrocenes ($E°$ = 0.94 V).

EXPERIMENTAL SECTION

General Procedures. All manipulations were performed under an inert atmosphere in a nitrogen filled MBraun Labmaster dp glovebox or using standard Schlenk techniques unless stated otherwise. Reagents were obtained from commercial sources. All solvents were dried using an MBraun controlled atmospheres solvent purification system and stored in Straus flasks under a N_2 atmosphere or over 4 Å molecular sieves in the glovebox. Chloroform-*d* was dried over calcium hydride, distilled prior to use, and stored in the glovebox over 4 Å molecular sieves. Acetonitrile-d_3 and CD_2Cl_2 were purchased from Cambridge Isotope Laboratories and stored in the glovebox over 3 Å or 4 Å molecular sieves, respectively. The syntheses of **S**$(OTf)_2$, CyDAB**Se**OTf_2, $Dipp_2$BIAN**Te**OTf_2, copper phthalimide, *N*-ferrocenyl pthalimide, and 2,6-pyridinedialdehyde were prepared *via* literature procedures.[25−30] Iodoferrocene and aminoferrocene were prepared using modified literature procedures. Proton, $^{13}C\{^1H\}$, $^{19}F\{^1H\}$, and $^{31}P\{^1H\}$ NMR spectroscopic data were collected on a 400 MHz Varian Inova spectrometer (399.762 MHz for ^1H; 100.52 MHz for ^{13}C; 376.15 for ^{19}F; 161.825 MHz for ^{31}P). NMR spectra were recorded at room temperature, unless otherwise indicated, in $CDCl_3$, CD_3CN, or CD_2Cl_2, and were referenced using the residual protons of the deuterated solvents ($CHCl_3$, δ_H = 7.26; CH_3CN, δ_H = 1.9, 3; DCM, δ_H = 5.30), coupling constants are listed in hertz. Carbon-12 NMR spectra were referenced using carbon signals from the respective solvent ($CHCl_3$, δ_C = 77.16(3); CH_3CN, δ_C = 1.32(7), 118.26(1); DCM, δ_C = 54.00(5)). Phosphorus-31$\{^1H\}$ and $^{19}F\{^1H\}$ NMR spectra were recorded unlocked relative to an external standard ($^{31}P\{^1H\}$, 85% H_3PO_4, δ_P = 0.00; $^{19}F\{^1H\}$, $CF_3C_6H_5$, δ_F = −63.9). Single crystal X-ray diffraction data were collected on a Nonius Kappa-CCD or a Bruker Apex II-CCD area detector using Mo Kα radiation (λ = 0.71073 Å). Crystals were selected under Paratone-N oil, mounted on MiTeGen micromounts or nylon loops, and then immediately placed in a cold stream of N_2. Structures were solved and refined using SHELXTL. UV/vis absorption spectra were recorded over a range of 235−800 nm using a Varian Cary 300 spectrometer in either CH_2Cl_2 (for **1Fc** and **1FcP**) or CH_3CN (for **1FcS**, **1FcSe**, and **1FcTe**). **1FcP** was measured at a concentration of 2.5×10^{-5} M, while all other compounds had a concentration of 2.0×10^{-5} M. FT-IR spectra were collected on samples as KBr pellets using a Bruker Tensor 27 spectrometer, with a resolution of 4 cm^{-1}. Samples for FT-Raman spectroscopy were packed in capillary tubes and flame-sealed. Data were collected using a Bruker RFS 100/S spectrometer, with a resolution of 4 cm^{-1}. Melting and decomposition points were recorded in flame-sealed capillary tubes using a Gallenkamp Variable Heater. High resolution mass spectrometry (HRMS) was collected using a Finnigan MAT 8200 instrument. Elemental analyses (C, H, N) were performed by Laboratoire d'Analyze Élémentaire de l'Université de Montréal, Montréal, QC, Canada. The electrochemical apparatus employed for cyclic voltammetry (CV) was an Autolab30 electrochemical workstation equipped with GPES 4.9 software. The working electrodes were either a glassy carbon (GC) electrode built from a Tokai GC-20 glassy carbon rod (3 mm diameter) or a platinum electrode built from a platinum wire (1 mm diameter), a Premion product purchased from Alfa Aesar. The disk electrode surfaces were prepared by polishing on silicon carbide papers (500, 1200, 2400, and 4000) and successively over diamond pastes (1 and 0.25 μm) from Struers. The working electrodes were stored in ethanol and, before using, were polished with diamond paste (1 μm), rinsed with dry ethanol, sonicated in dry ethanol for 5 min, and dried. The previous sequence with ethanol was then repeated using 0.25 μm diamond paste to start. Electrochemical activation of the disk electrode surfaces was carried out before each measurement by multicycling at 0.1 V s^{-1} in the background solution until stabilization of the capacitive current. The reference electrode was a Ag/AgCl, built by filling a glass tube closed at an extremity with a junction, in an CH_3CN/0.1 M $TBAPF_6$ solution. A silver wire was then immersed in the solution inside the glass tube, and the reference electrode was left to stabilize its potential for a week prior to use. All data are reported versus the standard calomel electrode (SCE). Introducing one molar equivalent of nitrobenzene to the electrochemical cell after each experiment allowed for the calibration to be made. The standard potential ($E°$) for the reversible reduction of nitrobenzene to its corresponding radical anion was calibrated toward ferrocene in a separate experiment. The $E°$ of ferrocene in DCM is established to be 0.644 V vs SCE.[31,32] The $E°$ of nitrobenzene in DCM was found to be −0.986 V vs SCE. The reversible reduction of nitrobenzene to its radical anion involves a single electron transfer; therefore, the intensity of the voltammetric peak was used to approximate the number of electrons exchanged in the electrochemical processes of the studied compounds. The counter-electrode was a platinum wire. All electrochemical measurements were carried out using the same set of electrodes.

The electrochemical measurements of compounds **1Fc**, **1FcS**, **1FcSe**, **1FcTe**, and **1FcP** were conducted in an in-house designed and built glass cell at room temperature. Due to the sensitivity of the compounds to ambient air, the experiments were performed inside of a glovebox. The electrochemical characterization of compounds **1Fc** and **1FcP** were carried out in a 5 mL DCM/0.1 M $TBAPF_6$ (tetrabutylammonium hexafluorophosphate) electrolyte solution containing the appropriate analyte (2 mM) and using the platinum electrode as a working electrode. The electrochemical characterization of compounds **1FcS**, **1FcSe**, and **1FcTe** were carried out in a 5 mL CH_3CN/0.05 M $TBABF_4$ (tetrabutylammonium tetrafluoroborate) electrolyte solution saturated with the analyte. For these measurements, the glassy C was used as the working electrode. For all measurements, feedback correction was employed to minimize the ohmnic drop between the reference and working electrode. The corresponding background curves were then subtracted from the CVs in order to eliminate the capacitive current contribution.

Synthesis. Iodoferrocene. A 500 mL Schlenk flask equipped with a large stir bar was charged under a nitrogen atmosphere with ferrocene (8.00 g, 0.043 mol), tBuOK (0.48 g, 0.0043 mol), and 300 mL of THF. The orange-yellow solution was cooled to −78 °C; some of the dissolved ferrocene precipitated during this process. Under rigorous stirring, 1.7 M tBuLi (25 mL, 0.043 mol) in *n*-hexane was added dropwise over 1 h. The addition was complete after 20 min, at which time the cold bath was removed and the reaction mixture was allowed to warm to room temperature, then stirred for an additional 2 h. The color of the reaction mixture changes from opaque orange to red-orange to a dark clear red. The reaction mixture was once again cooled to −78 °C, and under vigorous stirring, I_2 (12.00 g, 0.0473 mol) was added in one portion. The cold bath was removed, and the mixture was allowed to warm to room temperature. Stirring continued for 12 h. The mixture was then first diluted with 200 mL of Et_2O, then washed with portions of saturated aqueous Na_2SO_3 (2 × 100 mL) and H_2O (3 × 150 mL) and dried with $MgSO_4$. The solvent was removed by rotary evaporation to yield the crude product as a yellow-brown oil (8.62 g, 0.026 mol, 60%), which solidifies upon storing in a freezer overnight. Spectroscopic properties were in agreement with literature values.[33,34] Unreacted ferrocene was present in the crude product; however, its presence did not affect onward chemistry and was therefore used without further purification. The relative ^1H signal ratios (ferrocene/iodoferrocene) were examined in order to determine the amount of pure iodoferrocene per gram of crude solid to be used in future transformations.

Aminoferrocene. To a 500 mL round-bottom Schlenk flask, degassed, was added anhydrous ethanol (100 mL) to a slurry of *N*-ferrocenyl phthalimide[29] (5.99 g, 0.018 mol) and hydrazine monohydrate (0.873 mL, 0.018 mol). The clear yellow solution was refluxed under N_2 for 2.5 h. The mixture was then cooled to room temperature. Degassed H_2O was added (200 mL), and the product was extracted with Et_2O. The yellow organic layer was dried over $MgSO_4$ and the supernatant transferred to a Schlenk tube and evaporated *in vacuo* to dryness, yielding a bright yellow-orange powder (2.57 g, 0.012 mol, 68%). Impurities were removed by sublimation

dx.doi.org/10.1021/ic300974u | Inorg. Chem. 2012, 51, 8425−8432

under a dynamic vacuum at 60 °C (coldfinger at −15 °C). The product was stored under an inert atmosphere of N_2. Aminoferrocene prepared according to the above procedure showed spectroscopic properties consistent with those previously published.[35]

1Fc. Mixtures of aminoferrocene (1.91 g, 9.48 mol), degassed ethanol (50 mL), and 2,6-pyridinedialdehyde[30] (0.636 g, 4.72 mmol) were refluxed under an inert atmosphere for 12 h with constant stirring. The product was collected by filtration, washed with cold ethanol (2 × 50 mL), and dried *in vacuo* to give a fine dark red-purple powder (2.10 g, 4.20 mmol, 89%). ^{1}H NMR ($CDCl_3$, δ): 8.81 (s, 2H), 8.21 (d, 2H, $^3J_{H-H}$ = 7.6), 7.84 (t, 1H, $^3J_{H-H}$ = 7.6), 4.71 (pt, 4H, $^3J_{H-H}$ = 2.0), 4.35 (pt, 4H, $^3J_{H-H}$ = 2.0), 4.21 (s, 10H). ^{13}C{^{1}H} NMR ($CDCl_3$, δ): δ 62.62, 67.02, 68.77, 102.27, 120.66, 136.10, 154.11, 156.37. UV/vis (CH_2Cl_2): λ_{max} 319.9 nm. FT-IR (cm^{-1} (ranked intensity)): 1579(13), 1561(4), 1462(6), 1348(14), 1232(11), 1106(3), 1040(15), 1001(7), 962(8), 927(5), 804(1), 738(12), 523(10), 491(2), 456(9). FT-Raman (cm^{-1} (ranked intensity)): 1616(1), 1580(2), 1562(7), 1458(4), 1376(12), 1273(5), 1229(3), 1110(8), 990(6), 670(11), 642(14), 585(13), 334(10), 283(9), 162(15). Mp: 223−230 °C. Elem. anal. calcd for $C_{27}H_{23}N_3Fe_2$: C, 64.71; H, 4.63; N, 8.38. Found: C, 64.47; H, 4.67; N, 8.34.

1FcS. A solution of **1Fc** (150.0 g, 0.299 mmol) in DCM (3 mL) was added dropwise to a solution of $S(OTf)_2$[25] (0.076 g, 0.229 mmol) in DCM (3 mL) at room temperature. The product was precipitated by the addition of *n*-pentane (3 × 10 mL) and Et_2O (3 × 10 mL) and dried *in vacuo* to give a dark blue-green fine powder (0.133 g, 0.160 mmol, 70%). Single crystals were obtained *via* vapor diffusion of Et_2O in CH_3CN. ^{1}H NMR (CD_3CN, δ): δ 10.07 (s, 2H), 9.02 (d, 2H, $^3J_{H-H}$ = 7.8), 8.85 (t, 1H, $^3J_{H-H}$ = 7.8), 5.52 (*pt*, 4H), 5.18 (pt, 4H), 4.53 (s, 10H). UV/vis (CH_3CN): λ_{max} 260.0 nm. FT-IR (cm^{-1} (ranked intensity)): 3071(10), 1617(9), 1573(15), 1553(11), 1515(4), 1403(7), 1266(1), 1227(14), 1179(5), 1027(2), 817(8), 636(3), 574(12), 518(13), 484(6). FT-Raman (cm^{-1} (ranked intensity)): 1614(9), 1547(3), 1511(1), 1499(11), 1400(2), 1294(13), 1231(5), 1090(8), 1064(15), 1043(14), 628(4), 493(7), 296(3), 332(10), 120(12). Decomposition point: 120−130 °C. HRMS $C_{28}H_{23}N_3Fe_2S_2O_3F_3$ calcd (found): 681.9832 (681.9846).

1FcSe. A solution of **1Fc** (0.227 g, 0.453 mmol) in DCM (3 mL) was added dropwise to a solution of $CyDABSeOTf_2$[26] (0.266 g, 0.453 mmol). The product was then precipitated by the addition of *n*-pentane (3 × 10 mL) and Et_2O (3 × 10 mL) and dried *in vacuo* to give a dark green-blue powder (0.270 g, 0.308 mmol, 68%). Single crystals were obtained *via* vapor diffusion of Et_2O in CH_3CN. ^{1}H NMR (CD_3CN, δ): 10.14 (s, 2H), 8.94 (d, 2H, $^3J_{H-H}$ = 7.8), 8.85 (t, 1H, $^3J_{H-H}$ = 7.8), 5.55 (*pt*, 4H), 5.15 (pt, 4H), 4.52 (s, 10H). UV/vis (CH_3CN): λ_{max} 314.9 nm. FT-IR (cm^{-1} (ranked intensity)): 3058(13), 1607(10), 1573(12), 1549(9), 1512(3), 1407(7), 1267(1), 1221(15), 1169(6), 1028(4), 820(11), 635(2), 571(14), 513(8), 484(5). FT-Raman (cm^{-1} (ranked intensity)): 2005(15), 1608(10), 1549(2), 1512(1), 1407(3), 1241(4), 1222(6), 1085(13), 1035(12), 629(5), 495(9), 394(14), 324(11), 295(8), 285(7). Decomposition point: 205−212 °C. Elem. anal. calcd for $C_{29}H_{23}N_3Fe_2Se_1O_6S_2F_6$: C, 39.66; H, 2.64; N, 4.78; S, 7.30. Found: C, 38.97; H, 2.49; N, 4.76; S, 6.84.

1FcTe. **1Fc** (0.079 g, 0.157 mmol) in DCM (3 mL) was added dropwise to a solution of $Dipp_2BIANTeOTf_2$[27] (0.145 g, 0.157 mmol) in DCM (3 mL). The product was then immediately precipitated and washed by the addition of *n*-pentane (3 × 10 mL) and Et_2O (3 × 10 mL) and dried *in vacuo* to give a dark blue-green fine powder (0.095 g, 0.102 mmol, 65%). Single crystals were obtained *via* vapor diffusion of Et_2O in CH_3CN. ^{1}H NMR (CD_3CN, δ): δ 10.32 (s, 2H), 8.84 (d, 2H, $^3J_{H-H}$ = 7.8), 8.73 (t, 1H, $^3J_{H-H}$ = 7.8), 5.55 (*pt*, 4H), 5.07 (pt, 4H), 4.48 (s, 10H). UV/vis (CH_3CN): λ_{max} 255.0 nm. FT-IR (cm^{-1} (ranked intensity)): 3052(13), 1606(9), 1572(7), 1544(11), 1506(4), 1436(15), 1410(5), 1268(1), 1225(10), 1029(2), 797(6), 636(3), 572(8), 517(14), 484(12). FT-Raman: (cm^{-1} (ranked intensity)): 2137(13), 2000(14), 1571(15), 1543(2), 1508(1), 1409(3), 1241(4), 1220(5), 1067(12), 1029(8), 630(6), 497(10), 321(11), 296(7), 284(9). Decomposition point: 115−121 °C. HRMS $C_{28}H_{23}N_3Fe_2Te_1O_3S_1F_3$ calcd (found): 779.91737 (779.91706). Elem. anal. calcd for $C_{29}H_{23}N_3Fe_2Te_1O_6S_2F_6$: C, 37.58; H, 2.50; N, 4.53; S, 6.92. Found: C, 37.08; H, 2.19; N, 4.54; S, 6.31.

1FcP. A mixture of **1Fc** (0.150 g, 0.299 mmol) in DCM (3 mL) was added dropwise to a solution of PI_3 (0.123 g, 0.299 mmol) in DCM (3 mL) at room temperature and was allowed to stir for 10 min. The product was precipitated by the addition of *n*-pentane (3 × 10 mL) and Et_2O (3 × 10 mL) and dried *in vacuo* to give a dark green-black fine powder (0.218 g, 0.239 mmol, 80%). ^{1}H NMR (CD_3CN, δ): 9.52 (d, 2H), 8.63 (d, 2H, $^3J_{H-H}$ = 7.8), 8.12 (t, 1H, $^3J_{H-H}$ = 7.8), 5.52 (*pt*, 4H), 4.86 (pt, 4H), 4.57 (s, 10H). ^{31}P NMR (CD_3CN, δ): 123.99. UV/vis (CH_2Cl_2): λ_{max} 295.1 nm. FT-IR (cm^{-1} (ranked intensity)): 3081(7), 1628(14), 1459(15), 1407(8), 1375(10), 1335(4), 1242(11), 1104(6), 1025(3), 1001(13), 934(12), 820(2), 769(5), 708(9), 499(1). FT-Raman (cm^{-1} (ranked intensity)): 3101(10), 1627(6), 1572(2), 1497(9), 1451(5), 1373(7), 1239(4), 1105(12), 1055(11), 831(15), 641(3), 478(13), 298(8), 163(14), 110(1). Decomposition point: 228−233 °C. HRMS $C_{27}H_{23}N_3Fe_2P_1$ calcd (found): 532.03290 (532.03176). Elem. anal. calcd for $C_{27}H_{23}N_3Fe_2P_1I_3$: C, 35.52; H, 2.54; N, 4.60. Found: C, 35.55; H, 2.43; N, 4.78.

■ ASSOCIATED CONTENT

Supporting Information

^{1}H NMR spectra, CVs, UV−vis for all compounds, and a crystallographic file in CIF format. This material is available free of charge via the Internet at http://pubs.acs.org.

■ AUTHOR INFORMATION

Corresponding Author

*E-mail: pragogna@uwo.ca.

Notes

The authors declare no competing financial interest.

■ ACKNOWLEDGMENTS

The authors are very grateful to the Natural Sciences and Engineering Research Council of Canada (NSERC), the Canada Foundation for Innovation, Ontario Ministry of Research and Innovation, and UWO for generous financial support. We also thank J. W. Dube for assistance with X-ray crystallographic studies.

■ REFERENCES

(1) Martin, C. D.; Ragogna, P. J. *Annu. Rep. Prog. Chem.* **2011**, *107*, 110−124.

(2) Dutton, J. L.; Ragogna, P. J. *Coord. Chem. Rev.* **2011**, *255*, 1414−1425.

(3) *Ferrocenes: Ligands, Materials, and Biomolecules*; Stepnicka, P., Ed.; John Wiley & Sons Ltd: West Sussex, U. K., 2008.

(4) Atkinson, R. C. J.; Gibson, V. C.; Long, N. J. *Chem. Soc. Rev.* **2004**, *33*, 313−328.

(5) De Boer, M.; Eric, J.; Van Der Heijden, H.; Verhoef-Van Wijk, C.; Van Zon, A.; Company, S. O. U.S. Patent Ser. No. 10/208,535, 2002.

(6) Gibson, V. C.; Halliwell, C. M.; Oxford, P. J.; Smith, A. M.; White, A. J. P.; Williams, D. J. *Dalton Trans.* **2003**, 918−926.

(7) Multani, K.; Stanlake, L. J. E.; Stephan, D. W. *Dalton Trans.* **2010**, *39*, 8957−8966.

(8) Stanlake, L. J. E.; Stephan, D. W. *Dalton Trans.* **2011**, *40*, 5836−5840.

(9) Bildstein, B.; Malaun, M.; Kopacka, H.; Fontani, M.; Zanello, P. *Inorg. Chim. Acta* **2000**, *300−302*, 16−22.

(10) Gibson, V. C.; Long, N. J.; Oxford, P. J.; White, A. J. P.; Williams, D. J. *Organometallics* **2006**, *25*, 1932−1939.

(11) Gregson, C. K. A.; Gibson, V. C.; Long, N. J.; Marshall, E. L.; Oxford, P. J.; White, A. J. P. *J. Am. Chem. Soc.* **2006**, *128*, 7410−7411.

(12) Reeske, G.; Cowley, A. H. *Chem. Commun.* **2006**, 1784−1786.

(13) Reeske, G.; Cowley, A. H. *Chem. Commun.* **2006**, 4856−4858.

(14) Martin, C. D.; Ragogna, P. J. *Inorg. Chem.* **2012**, *51*, 2947−2953.
(15) Singh, A. P.; Roesky, H. W.; Carl, E.; Stalke, D.; Demers, J.-P.; Lange, A. *J. Am. Chem. Soc.* **2012**, *134*, 4998−5003.
(16) Baker, R. J.; Jones, C.; Kloth, M.; Mills, D. P. *New J. Chem.* **2004**, *28*, 207−213.
(17) Bruce, M.; Gibson, V. C.; Redshaw, C.; Solan, G. A.; White, A. J. P.; Williams, D. J. *Chem Commun.* **1998**, 2523−2524.
(18) Scott, J.; Gambarotta, S.; Korobkov, I.; Knijnenburg, Q.; de Bruin, B.; Budzelaar, P. H. M. *J. Am. Chem. Soc.* **2005**, *127*, 17204−17206.
(19) Knijnenburg, Q.; Smits, J. M. M.; Budzelaar, P. H. M. *Organometallics* **2006**, *25*, 1036−1046.
(20) Jurca, T.; Lummiss, J.; Burchell, T. J.; Gorelsky, S. I.; Richeson, D. S. *J. Am. Chem. Soc.* **2009**, *131*, 4608−4609.
(21) Jurca, T.; Dawson, K.; Mallov, I.; Burchell, T.; Yap, G. P. A.; Richeson, D. S. *Dalton Trans.* **2010**, *39*, 1266−1272.
(22) Martin, C. D.; Le, C. M.; Ragogna, P. J. *J. Am. Chem. Soc.* **2009**, *131*, 15126−15127.
(23) Martin, C. D.; Ragogna, P. J. *Dalton Trans.* **2011**, *40*, 11976−11980.
(24) Pauling, L. *The Nature of the Chemical Bond*; Cornell University Press: Ithaca, NY, 1960.
(25) Martin, C. D.; Ragogna, P. J. *Inorg. Chem.* **2010**, *49*, 4324−4330.
(26) Dutton, J. L.; Battista, T. L.; Sgro, M. J.; Ragogna, P. J. *Chem. Commun.* **2010**, *46*, 1041−1043.
(27) Dutton, J. L.; Tuononen, H. M.; Ragogna, P. J. *Angew. Chem., Int. Ed.* **2009**, *48*, 4409−4413.
(28) Bildstein, B.; Malaun, M.; Kopacka, H.; Wurst, K.; Mitterbock, M.; Ongania, K.-H.; Opromolla, G.; Zanello, P. *Organometallics* **1999**, *18*, 4325−4336.
(29) Montserrat, N.; Parkins, A. W.; Tomkins, A. R. *J. Chem. Res. Synop.* **1995**, *8*, 336−337.
(30) Britovsek, G. J. P.; Bruce, M.; Gibson, V. C.; Kimberley, B. S.; Maddox, P. J.; Mastroianni, S.; McTavish, S. J.; Redshaw, C.; Solan, G. A.; Strmberg, S.; White, A. J. P.; Williams, D. J. *J. Am. Chem. Soc.* **1999**, *121*, 8728−8740.
(31) Sauro, V.; Magri, D. C.; Pitters, J. L.; Workentin, M. S. *Electrochem. Acta.* **2010**, *55*, 5584−5591.
(32) Tsierkezos, N. G. *J. Solution Chem.* **2007**, *36*, 289−302.
(33) Kamounah, F. S.; Christensen, J. B. *J. Chem. Res. (S)* **1997**, 150.
(34) Goeltz, J. C.; Kubiak, C. P. *Organometallics* **2011**, *30*, 3908−9010.
(35) Butler, D. C. D.; Richards, C. J. *Organometallics* **2002**, *21*, 5433−5436.